Effects of Neutral Density on Electron Temperature and Mobility in a Crossed-field Trap

Emily C. Fossum* and Lyon B. King,†
Michigan Tech University, Houghton, MI, 49931

An electron trapping apparatus was constructed to emulate the electric and magnetic fields found in a Hall-effect thruster in order to investigate cross-field electron mobility. Anomalous mobility was previously observed in this device that is orders of magnitude higher than classical. The focus of this manuscript is to investigate the effect of neutral density on the electron temperature and cross-field mobility in the electron trap. It was found that electron temperature decreases with increasing neutral density. When electron temperature is taken into account in the calculation of classical mobility, trends are observed in this device that resemble classical scaling with neutral density; however, the magnitude of the observed mobility is 100 to 1,000 times higher than classically predicted. On further investigation of the electron temperature, it is determined that in some cases the electron temperature is much higher than would be possible if collisions were responsible for transport, as inelastic collisions, which prevail at higher electron energies, would cause electron cooling that is not seen here. Furthermore, an examination of the probe I-V characteristic reveals that the electron distribution function is highly non-Maxwellian in these cases, supporting a collisionless anomalous mobility.

Nomenclature

B_r	=	radial magnetic field
$\mathbf{B}$	=	magnetic field vector
B	=	magnitude of $\mathbf{B}$
$\mathbf{c}$	=	thermal velocity
e	=	elementary charge
$\mathbf{E}$	=	electric field vector
E_z	=	axial electric field
ϕ_p	=	plasma potential
ϕ_t	=	trap depth
J_a	=	current density at the anode
J_{ez}	=	cross-field electron current density
J_p	=	probe current density
k_B	=	Boltzmann constant, $1.3806503 \times 10^{-23}$ $m^2kg/(s^2K)$
m_e	=	electron mass
μ_{ez}	=	cross-field electron mobility
n_e, n_∞	=	electron number density
n_0	=	neutral particle density
ν_{ne}	=	electron-neutral collision frequency
ω_{ce}	=	electron gyro-frequency
σ	=	electron-neutral collision cross-section
T_e	=	electron temperature
$T_{e,\,exp}$	=	experimentally determined electron temperature
$\bar{v}_e$	=	average electron velocity
V_p	=	probe voltage

* Graduate Research Assistant, Mechanical Engineering, 815 R. L. Smith Bldg.
† Associate Professor, Mechanical Engineering, 815 R. L. Smith Bldg.

I. Introduction

HALL thrusters are highly efficient in-space propulsion devices with capabilities for satellite station keeping, orbit correcting, and orbit raising[1]. The defining characteristic of Hall thrusters is the crossed axial electric and radial magnetic fields. The electric field accelerates ionized gas from the thruster, which produces thrust, whereas the radial magnetic field sustains the electric field by impeding the highly mobile electron flow to the anode[2]. The criteria of the *E*- and *B*-field is such that the electron gyro-radius is small compared with apparatus dimensions while the gyro-radius and mean free path for ions are larger than apparatus dimensions; these criteria are necessary so that ions are only affected by the electric field, where the electron trajectories are controlled by both electric and magnetic fields. The crossed *E*- and *B*-fields induce the confining **E**x**B** electron drift, or Hall current, which holds electrons in azimuthal orbits around the discharge channel annulus. By classical theory, electrons are held in these orbits, and the only mechanism for motion across B-field lines toward the anode is momentum-transfer collisions with un-ionized propellant atoms. Given the case of a large Hall parameter, the cross-field electron mobility in radial magnetic (B_r) and axial electric (E_z) fields reduces to[3]:

$$\mu_{ez} = \frac{\nu_m}{B_r \omega_{ce}} \tag{1}$$

However, experimentally the electron mobility in Hall thrusters has been measured to be much larger than can be predicted by classical theory alone[4-11], at times 2-3 orders of magnitude higher. A detailed knowledge of the mechanisms responsible for anomalous mobility could prove useful in creating a more efficient thruster (as excess mobility can affect thruster efficiency) and would allow more accurate numerical models of the thruster discharge. Numerous electron mobility investigations are ongoing[12-19].

The approach in the current investigation is to reproduce key physical attributes of a Hall thruster in a greatly simplified environment. Dielectric wall effects, which are largely unknown in Hall thruster research[20, 21], have been removed by trapping a non-neutral plasma using electric and magnetic fields alone. The electric field is created and controlled externally through parallel plates in vacuum rather than via a self-consistent plasma. The electron density is limited in order to uncouple the plasma from the electric field, as a very low-density electron plasma has negligible space charge in comparison to applied fields. These characteristics enable in-situ probe diagnostics to determine internal plasma properties such as electron temperature and density, without the need for optical or fast-scanning diagnostic techniques[22,23]. While non-neutral plasma studies have not been documented in Hall thruster investigations, studies of non-neutral plasmas have proven to be useful for numerous types of charged particle transport experiments[24-30].

In past experiments with this device, the electron mobility was observed to be significantly higher than classical mobility[31] [40]. In addition to the disagreement in magnitude, the mobility scaling trends appeared to be non-classical with changes in magnetic and electric fields and neutral density. The focus of this manuscript is to investigate the mobility scaling with neutral density; an investigation of electric and magnetic field scaling will be addressed in future work. A linear dependence on neutral density is expected from the linear scaling of mobility with collision frequency. The classical scaling of mobility with neutral density is $\mu \sim n_0$, whereas the experimental mobility observed in the trap appeared to be non-classical, with $\mu \sim n_0^{0.5-0.9}$. In this past work an estimated electron temperature was used to calculate the theoretical classical mobility based on the total energy available to electrons traversing through the trap from anode to cathode. The electron temperature was assumed to vary with anode-to-cathode voltage and position within the trap, as these determine the total energy available, however temperature was assumed to be constant with all other trap operating parameters. Classical mobility scales with $\sqrt{T_e}$ because of the linear dependence on collision frequency where

$$\nu_{ne} = n_0 \sigma \bar{v}_e = n_0 \sigma \sqrt{\frac{8 k_B T_e}{\pi m_e}}. \tag{2}$$

If electron temperature within this trap varies with neutral density, this would change the expected scaling of mobility with neutral density. The goal of this manuscript is to investigate the effects of neutral density on both the electron temperature and mobility observed in the electron trap. Techniques are presented for in-situ electron temperature measurements, and mobility and electron temperature are measured in response to changes in neutral

density. Mobility, μ_{ez}, is a function of T_e, and if T_e can no longer be considered a variable independent of neutral density, the expected scaling with neutral density must be adjusted to reflect this.

II. Experimental Setup

A. Electron Trap

The electron trapping apparatus was described in detail in Ref. 41 and is shown in Fig. 1. The trap is much larger than a Hall thruster and has a 400-mm O.D. in order to operate over a large range of magnetic fields while maintaining scaling parameters, which are that $r_L << L$ where r_L is the electron Larmor radius and L is a characteristic length of the trap. A radial magnetic field was created with a shape and strength that is similar to that of a Hall thruster through use of magnetic windings on inner and outer magnetic poles. An axial electric field was created via parallel plate electrodes in vacuum. Carefully shaped electrodes were employed to ensure that electric equipotentials coincided with magnetic field lines within the trap volume, which emulates the quasi-neutral plasma potential structure found in a Hall thruster[32]. The axial electric field, formed self-consistently in the neutral plasma of a Hall thruster, is replicated in this apparatus by parallel plates in vacuum. The space-charge field due to the trapped one-component plasma is made negligible by adjusting the electron density within the trap to be less than $1x10^{10}$, such that the applied electric field can be assumed rigid and independent of plasma parameters[31]. Thus, the electric field is assumed rigid and known.

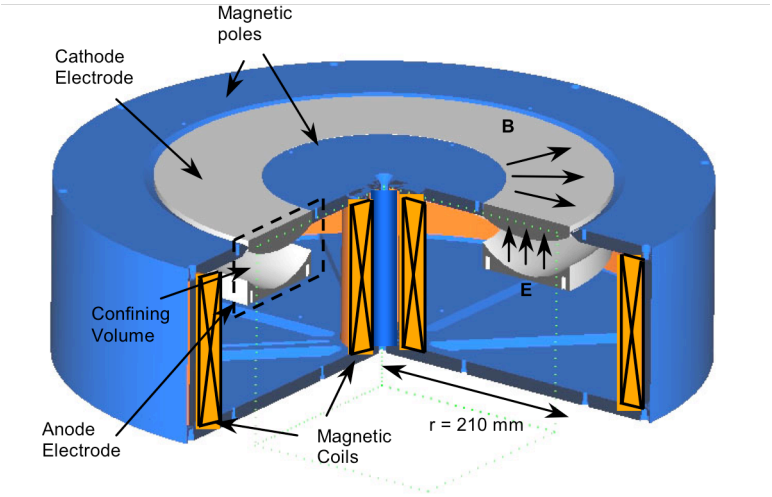

Fig. 1. A cutaway drawing of the electron trapping apparatus. The iron pole pieces are shown in blue and the radial magnetic field is created through windings (shown in orange) at the inner and outer pole pieces. The axial electric field is set up through two parallel plates (shown in gray) indicated as the anode and cathode.

Radial confinement is provided by an electrostatic force at the inner and outer radii, which is slightly enhanced by a weak magnetic mirror force due to increasing B_r at the iron poles. The electrostatic confining force acting at the inner and outer radii of the trap exists because of the departure of electrostatic equipotentials from magnetic field lines. This is illustrated in Fig. 2, where the electric equipotential field lines are shown with magnetic field lines superimposed (solved numerically using the electric-magnetic field solver, Maxwell®[33]). Since electrons are constrained to follow *B*-field lines (between collisions), they have a point of minimum potential energy at the center of the confining volume where the *B*-field is coincident with the electric equipotentials. As an electron travels from this region towards either edge of the confinement volume, the electric potential increases as the magnetic field lines depart from the electric equipotentials. The *B*-field lines passing through the confinement volume terminate on the iron pole pieces which are held at cathode potential, thus the total potential increase from trap center to trap edge along a *B*-field line (where the magnetic field lines intersect the pole) is the value of the local potential along that line at trap center with respect to the cathode. This is also equal to the total energy available to electrons as they gain energy traversing axially from the cathode, assuming electrons are emitted with negligible energy at the cathode (see section II.B.1.). The total electron energy is distributed over all directions and thus the energy in the direction parallel to the radial magnetic field is always less than the well depth, and confinement is very effective. Consider, for instance, an electron constrained to the *B*-field line that is coincident with the 60-V equipotential at the location

of the electrostatic probe in Fig. 2. In order to impact the iron pole at the trap periphery, the electron must climb a 60-V potential hill because the electron is constrained to the magnetic field line. Therefore, an electron on the field line at 60 V in the center of the confining volume would be in a 60-eV electrostatic potential well. It is clear, then, that the trapping depth of the electrostatic potential well on any magnetic field line can be easily determined and is equal to the potential difference between the cathode and the local potential on the magnetic field line at the trap center. There will be a depletion of the very-high-energy Maxwellian tail of the distribution, as the potential well has a finite depth; electrons with energy greater than this well depth will be lost at magnetic pole surfaces. The confinement properties of the electron trap are described in greater detail elsewhere[31].

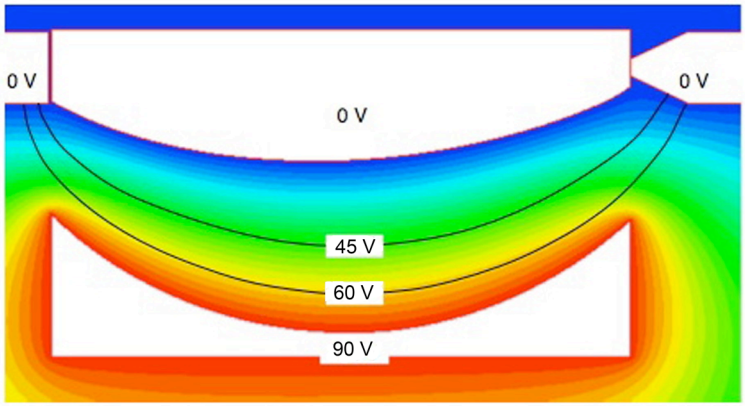

Fig 2. Electric equipotential contours of the confinement volume cross-section with magnetic field lines superimposed (solid black). Local potentials are indicated in text on the figure.

The trap is operated in the Isp Lab's Vacuum Test Facility #2, a 2-m-diameter, 4-m-long cylindrical vacuum chamber, providing a base pressure below 10^{-6} Torr. In order to obtain a local measure of neutral density inside the trapping volume a hot-cathode ionization gauge is mounted directly to the electron trap by a Conflat half-nipple welded to the back magnetic plate. Ionization gauge readings were taken before and after mobility measurements while no power was supplied to the magnets, electrodes, or filament in order to gain an accurate pressure reading. During trap operation the ionization gauge was disabled in order to eliminate any effects on mobility measurements. Argon was introduced within the vacuum chamber as background gas to vary the base pressure from ~10^{-6} to 10^{-4} Torr. Argon's higher ionization potential (15.8 eV) when compared to xenon (12.1 eV), the typical propellant used in Hall thrusters, reduces the undesired effects of ionization in this study. As long as the collision cross-sections of the background species is known[34], the background species has no bearing on the results of these mobility studies. The use of helium or neon as a background gas would further reduce ionization effects, and future tests are planned to utilize these in mobility studies as well.

B. Trap Operation and Diagnostics

1. Trap Loading

Electrons are injected into the trap using a thermionically-emitting thoriated-tungsten filament placed entirely inside the trap at one azimuthal location on the cathode surface. A filament heater circuit was isolated with an isolation transformer and was initially biased negatively with respect to the cathode. An I-V characteristic was taken measuring emission current in response to filament bias. In order to emit low energy electrons, the filament bias was tuned ~100-500 mV below the potential where no emission current was observed. This procedure introduces electrons to the trap with initial energy less than 0.5 eV and a thermal spread less than 1 eV[35]. The emission current, and hence the electron density within the trap, can be controlled by varying the filament heater current without significantly affecting the energy of emitted electrons.

2. Measuring Mobility

The transverse mobility, μ_{ez}, is related to the axial current flux, J_{ez} by $J_{ez} = en_e\mu_{ez}E_z$, where n_e is the electron density and E_z is the axial E-field. Because the axial field is known, we need only measure the anode current density, J_{ez}, and the electron density, n_e, in order to experimentally quantify mobility. We compute J_{ez} by measuring the

anode current and surface area. Electron density is derived using the probe theory described in Section III.B.3. to interpret current measured from an in-situ probe. Mobility can be described by

$$\mu_{ez} = \frac{J_{ez}}{en_e E_z} \sim \frac{J_a}{J_p} \tag{3}$$

where mobility is approximately proportional to the ratio of the anode current density, J_a, to the probe current density, J_p when the probe is held at local potential. Mobility was measured in response to electric and magnetic fields and neutral density. Five neutral density conditions were tested in random order and the entire test matrix of electric and magnetic field conditions was randomized at each neutral density condition to remove temporal and/or uncontrollable systematic effects.

3. Probe Diagnostics

A planar Langmuir probe was used to measure electron temperature and density. The probe collecting surface was aligned normal to the magnetic field lines so that it may be sensitive to the thermal electron motion parallel to the magnetic field. For the non-neutral electron plasma under study here, considerations are made that deviate from traditional probe theory [36] in quasi-neutral plasmas as the ion density is sufficiently low and the current to the probe is primarily electron current. In the present configuration the electron density and temperature can be found by examining the retarding region of the I-V characteristic (i.e. $V_p < \phi_p$, where V_p and ϕ_p are probe and plasma potential, respectively) similar to the analyses found in Refs. 37 and 38. Assuming that the plasma is in thermal equilibrium, the Maxwell-Boltzmann distribution of the plasma is given by

$$f = n_\infty \left(\frac{\beta}{\pi}\right)^{3/2} e^{-\beta(c_1^2 + c_2^2 + c_3^2)} \tag{4}$$

where n_∞ is the electron density in absence of a probe and $\beta = m_e/(2k_B T_e)$. The current flux to the probe is then given by

$$J_p = e\int_{-\infty}^{\infty} dv_1 \int_{-\infty}^{\infty} dv_2 \int_{v_{3,\min}}^{\infty} v_3 f(\mathbf{v}) dv_3 = en_\infty \sqrt{\frac{\beta}{\pi}} \int_{v_{3,\min}}^{\infty} v_3 e^{-\beta c_3^2} dv_3 \tag{5}$$

where v_i is the i-th component of the total velocity, and v_3 is the velocity component perpendicular to the probe collection surface, and $v_{3,min}$ is the minimum velocity an electron can have and still be collected by the probe. In this case, v_i is equivalent to c_i since there is no net flow of electrons parallel to the B-field and all motion is random thermal motion. Integrating equation (7) gives the current density to the probe as a function of probe voltage:

$$J_p = \frac{1}{4} en_\infty \bar{v}_e e^{-e(\phi_p - V_p)/k_B T_e} \tag{6}$$

Equation (6) can be used as a fit in the retarding region of the I-V probe characteristic in order to determine electron density and electron temperature parallel to the magnetic field. An isotropic assumption would need to be made to infer a three-dimensional average electron kinetic energy and average electron velocity.

III. Results

A. Electron Temperature

The probe I-V characteristic and curve fit described above was used to measure electron temperature in response to changes in electric and magnetic field and background neutral density. Fig. 3 shows characteristic probe traces for two different neutral density conditions at an electric field of 2.9×10^3 V/m and magnetic field of 90 G. The local potential at the probe is shown as a dotted line and the curve fit was used in the retarding region of the I-V characteristic. A temperature of 29.7 eV was found for the 2.3×10^{17} m^{-3} case and a cooler temperature of 10.3 eV was found from the 2.3×10^{18} m^{-3} case. Temperature versus neutral density is shown in Figure 4 indicating that

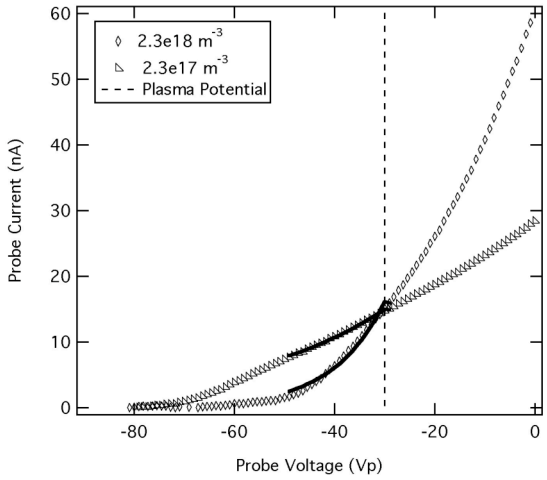

Fig. 3. Probe I-V Characteristics for the pressure conditions indicated in the legend for an electric field of 2.9×10^3 V/m and magnetic field of 90 G.

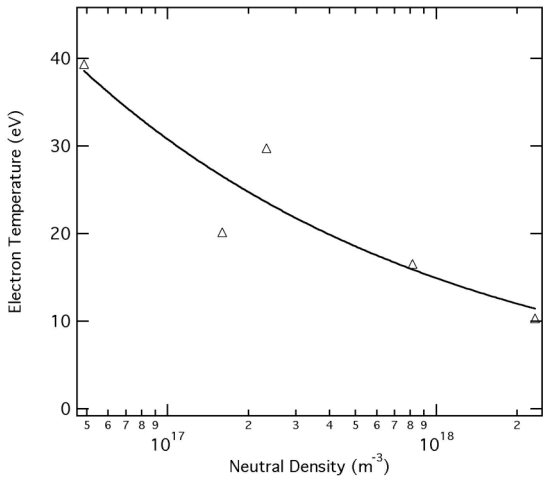

Fig. 4. Electron temperature versus neutral density for an electric field of 2.9×10^3 V/m and magnetic field of 90 G.

electron temperature decreases with increasing neutral density. A power-law curve fit indicates that electron temperature scales as $T_e \sim n_0^{-0.31}$, shown as a solid line in Figure 4.

Electron temperature versus E_z is shown in Figure 5 for five neutral density conditions. At the lowest neutral density conditions the electron temperature corresponds to an energy that is in some cases much higher than the excitation and ionization energies of argon (11.5 eV and 15.8 eV, respectively). At higher neutral density conditions the electron temperature is quenched to values below 20 eV. The maximum total energy available to electrons at the probe is the total depth of the trap, ϕ_t, (described in Section II.A.) which corresponds to a kinetic energy of $3kT/2$. Therefore, the electron temperature possible in the trap must be lower than $2\phi_t/3$ since a higher temperature corresponds to particles with energy greater than that which can be confined by the electrostatic well. The maximum allowable temperature of $2\phi_t/3$ is shown as a dotted line in Figure 5. The measured electron temperature for all conditions tested falls below this value.

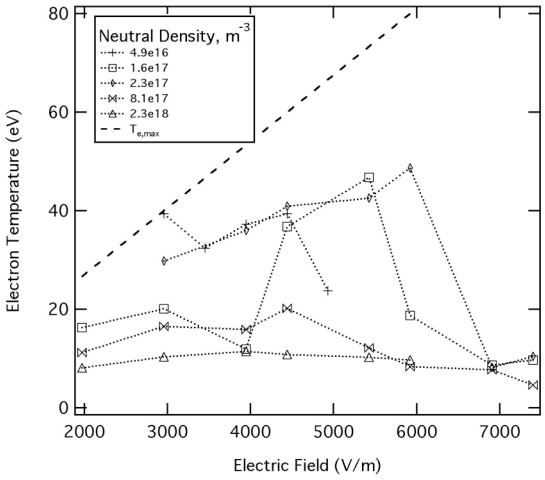

Fig. 5. Electron temperature versus electric field for various neutral density conditions. The theoretical maximum allowable temperature is shown as a dashed line.

B. Mobility Scaling With Neutral Density

Mobility was measured in response to background neutral (argon) density. The measured mobility is shown in Figure 6 at a magnetic field of 90 G and electric field of 2.9×10^{-3} V/m. The classical mobility is shown in Figure 6 as well, where the calculation for classical mobility incorporates the experimentally determined T_e at each neutral density condition, that is:

$$\mu = \frac{n_0 \sigma \sqrt{\frac{8kT_{e,\,exp}}{\pi m}}}{B_r \omega_{ce}} \tag{7}$$

A power-law curve fit for both experimental and theoretical mobility is shown in Figure 6. With the incorporation of the measured electron temperature, classical mobility scales as $\mu_{ez} \sim n_0^{0.90}$ and experimental mobility scales as $\mu_{ez} \sim n_0^{0.91}$.

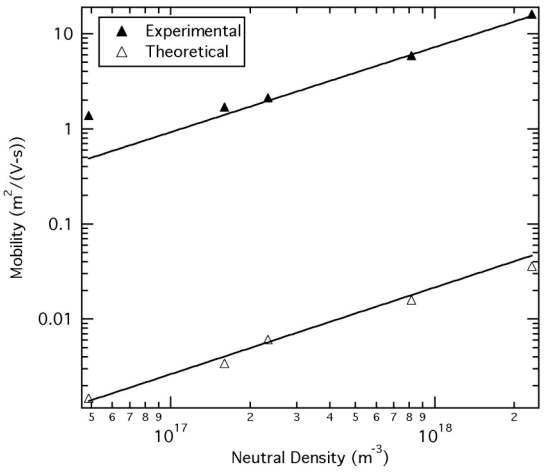

Fig. 6. Mobility versus neutral density for an electric field of 2.9×10^3 V/m and a magnetic field of 90 G

IV. Analysis

It was found that mobility in this device does not scale 1:1 with neutral density, which classical theory would suggest. However, electron temperature was found to decrease with increasing neutral density. Classical mobility scales linearly with $\sqrt{T_e}$ and T_e and n_0 are clearly not independent. Therefore, in examining the trends of mobility with neutral density, n_0, when changes in electron temperature are taken into account over the range of neutral densities investigated, the scaling agrees well with classical mobility. In the example shown in Figure 6, experimental mobility scales as $\mu_{ez} \sim n_0^{0.90}$ and classical mobility scales as $\mu_{ez} \sim n_0^{0.91}$, which both show a scaling of mobility that is less than 1:1 with neutral density.

Even though the scaling with n_0 appears to be classical, the experimental mobility remains 2-3 orders of magnitude higher than classical mobility. This alone suggests that a mechanism for cross-field transport exists that does not require electron-neutral collisions. Furthermore, several experimental observations support the existence of a collisionless mobility, in particular, the measured electron temperature and the probe I-V characteristics. The following observations suggest non-classical behavior: 1.) excessively high electron temperature 2.) variation of electron temperature with neutral density 3.) non-Maxwellian distribution indicated by probe traces. These observations are outlined below explaining why each suggests collisionless mobility.

At low neutral density, the measured electron temperature is much higher than would be expected if collisions alone were responsible for the cross-field mobility. An electron starts at the cathode with very low energy (ref. Section II.B.1. on trap loading). Each collision an electron suffers allows the electron to move axially toward the anode resulting in an increase in electron kinetic energy as the particle absorbs the potential energy of the field. If these collisions are elastic, the large mass difference between an electron and neutral will cause negligible change to the electron's kinetic energy. An electron will continue to gain energy (and thus increase temperature) with each collision as it moves across the magnetic field. However, once an electron has achieved an amount of energy equal to or greater than the excitation and/or ionization threshold there is a high probability that the next collision will result in an excited neutral or ion and the electron, while moving closer to the anode and gaining field energy, will also lose an amount of energy equal to the excitation or ionization potential. Because the excitation/ionization energy is larger than the random-walk field energy gained by the electron from the event, collision-induced mobility should produce a population of electrons whose average kinetic energy is limited to a value similar to the ionization potential (15.8 eV), corresponding to a temperature of 10 eV. In other words, inelastic collisions tend to reduce the electron temperature to a value below the excitation/ionization threshold. In the case of 90V potential difference between the cathode and anode, the probe is positioned 2/3 of the distance between the cathode and anode, so the total kinetic energy that can be gained by electrons is 60 eV; assuming isotropic energy distribution this corresponds to a maximum temperature of 40 eV at this location. At higher neutral densities the cooling behavior described above is observed where the electrons are seen to have a temperature of only 10-20 eV after falling through an electrostatic potential of 60 V, suggesting frequent collisions with argon neutrals. However, at low neutral density, the measured electron temperature corresponds to an energy that is much higher than the excitation and ionization energies of argon. Because very little cooling is observed, the high electron temperature in the low-neutral-density conditions suggests that electrons have suffered few collisions with argon neutrals and, instead, have traveled the distance from cathode to probe location through some collisionless mechanism.

An argument can be made that, given purely classical mobility, electron temperature should be constant with neutral density; conversely, if electron temperature is found to vary with neutral density, a non-classical mobility is present that does not rely on electron-neutral collisions. The number of total collisions required to traverse a given distance across the magnetic field is fixed by the Larmor radius, regardless of how often collisions take place,

assuming electrons are magnetized (large Hall parameter). At constant electric field, the total energy available to electrons is fixed as well. Electrons lose a certain amount of energy through inelastic collisions with neutrals (described above), which is dependent on incident electron energy; incident energy is determined by the energy gained from the electric field and thus energy losses are also fixed by the field conditions. Therefore, the net energy gain is independent of collision frequency, since both the total number of collisions and the energy gain and loss for an electron moving through the trap are fixed by the field conditions. In other words, the collision frequency would only affect the total residence time of electrons in the trap, but collision frequency would not affect the total energy gain and collisional cooling effects as an electron traverses through the trap. (In the limit of complete vacuum where collision frequency is zero, an electron will not move through the trap and will remain indefinitely.) Therefore, if collisions are solely responsible for cross-field mobility, electron temperature will be constant with collision frequency and hence neutral density. However, in the case of collisionless or anomalous mobility, electron temperature could be dependent on electron-neutral collision frequency. To illustrate this, consider a mechanism for cross-field electron mobility that allows electrons to traverse the trap in complete absence of neutrals (vacuum condition). The time-of-flight required to travel from cathode-to-anode would be finite regardless of collision frequency (in contrast to collisional mobility where time-of-flight would be infinite in the absence of collisions). The presence of neutrals would, however, affect the temperature of the electrons because of collisional cooling; the degree to which electrons are cooled depends on the number of collisions an electron encounters while moving through the trap. In the limit of absolute vacuum an electron experiences no collisions and gains the maximum amount of energy from the field, displaying a high electron temperature. In the case of low neutral density, electrons are cooled as they suffer collisions during their journey; as neutral density increases the amount of cooling would increase, showing a decrease in T_e as n_0 is increased. It follows then that the observed variation of electron temperature with neutral density is consistent with a mobility mechanism that does not require electron-neutral collisions.

Finally, when examining the I-V probe characteristics where the highest temperatures were measured, the electron energy distribution appears to be highly non-Maxwellian. As previously described, the trap has a finite well depth, $\phi_t = 3kT/2$, so that electrons with energy greater than this depth are lost to the poles, resulting in a depletion of the high-energy Maxwellian tail of the energy distribution. Because of equipartition of energy, where the average kinetic energy in any direction is $kT/2$, this depletion will appear at $\phi_t/3$ in a one-dimensional electron energy distribution captured by the planar probe. Collisions would cause energy relaxation of the truncated Maxwellian to an overall lower temperature. In the lowest neutral density cases, where the highest electron temperatures were observed, at retarding voltages greater (i.e. more negative) than 1/3 the trap depth, the probe characteristic demonstrates a steep drop-off which is indicative of depletion of electrons above this energy. This characteristic shown in Figure 7 suggests very little energy relaxation of the energy distribution function, in contrast to the highest neutral density cases (as shown by the highest pressure case in Figure 3), where the trace appears Maxwellian. Collisions responsible for the energy relaxation in the low neutral density case are absent further supporting the existence of cross-field mobility that does not rely on electron-neutral collisions.

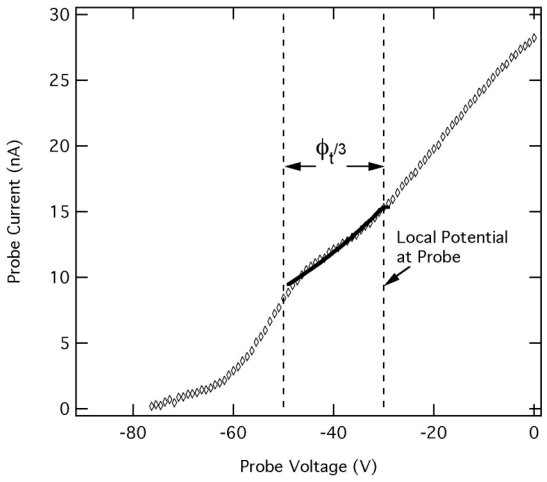

Fig. 7. Probe I-V characteristic for the lowest neutral density of 4.9×10^{16} m^{-3} showing the non-Maxwellian energy distribution.

V. Conclusions

This paper presents a description of an apparatus that can be used to investigate certain mechanisms responsible for electron mobility. The first stage of this research was to measure mobility in the electron trap and compare it to

the classical mobility model. In previous work, cross-field mobility was observed that was up to three orders of magnitude higher than the classical prediction. By classical theory, mobility should scale 1:1 with neutral density; the scaling of mobility with neutral density in this device has been found to be less than 1:1. However, electron temperature was found to decrease with increasing neutral density and cannot be considered as a variable independent of neutral density, which was previously assumed. Taking the electron temperature into account in the determination of classical mobility, the experimental mobility scaling with neutral density has been found to be consistent with classical scaling. However, the order of magnitude of experimental mobility suggests that an anomalous mobility is present that does not depend on electron-neutral collisions. Support for a collisionless mobility is provided by the excessively high electron temperature, the electron temperature variation with neutral density, and the non-Maxwellian distribution indicated by the probe traces. Therefore, it is determined that mobility with neutral density scaling appears classical but there is an anomalous contribution that is independent of electron-neutral collisions.

References

[1]F. S. Gulczinski, III. and R. A. Spores, "Analysis of Hall-effect thrusters and ion engines for orbit transfer missions," presented at the 32nd AIAA Joint Propulsion Conference, Lake Buena Vista, Fla., 1996, AIAA-1996-2973.

[2]V. V. Zhurin, H. R. Kaufman, and R. S. Robinson, "Physics of closed drift thrusters," *Plasma Sources Sci. Technol.*, 8, 1999, pp. R1.

[3]F. F. Chen, *Introduction to Plasma Physics and Controlled Fusion, 2nd Edition,* Plenum Press, New York, 1984.

[4]G. S. Janes, and R. S. Lowder, "Anomalous electron diffusion and ion acceleration in a low-density plasma," *Phys. Fluids*, 9 (6), 1966, pp. 1115-1123.

[5]N. B. Meezan, W. A. Hargus, and M. A. Cappelli, "Anomalous electron mobility in a coaxial Hall discharge plasma," *Phys. Rev. E*, 63, 2001, pp. 026410.

[6]J. P. Boeuf, and L. Garrigues, "Low frequency oscillations in a stationary plasma thruster," *J. Appl. Phys.*, 84 (7), 1998, pp. 3541.

[7]G. Guerrini, and C. Michaut, "Characterization of high frequency oscillations in a small Hall-type thruster," *Phys. Plasmas*, 6, 1999, pp. 343.

[8]N. Gascon and M. A. Cappelli, "Plasma instabilities in the ionization regime of a Hall thruster," presented at the 39th AIAA Joint Propulsion Conference, Huntsville, Alabama, 2003, AIAA-2003-4857.

[9]E. Y. Choueiri, "Plasma oscillations in Hall thrusters," *Phys. Plasmas*, 8 (4), 2001, pp. 1411.

[10]I. D. Kaganovich, Y. Raitses, D. Sydorenko, and A. Smolyakov, "Kinetic effects in a Hall thruster discharge," *Phys. Plasmas*, 14, 2007, pp. 057104.

[11]M. Keidar, I. D. Boyd, and I. I. Beilis, "Plasma flow and plasma – wall transition in Hall thruster channel," *Phys. Plasmas*, 8 (12), 2001, pp. 5315.

[12]R. Spektor, "Quasi-linear analysis of anomalous electron mobility inside a Hall thruster," presented at the 30th International Electric Propulsion Conference, Florence, Italy, 2007, IEPC-2007-70.

[13]J. L. Rovey, M. P. Giacomi, R. A. Stubbers, and B. E. Jurczyk, "A planar Hall thruster for investigating electron mobility in ExB devices," presented at the 30th International Electric Propulsion Conference, Florence, Italy, 2007, IEPC-2007-187.

[14]G. Coduti *et al.*, "Investigation of electron transport properties in Hall thrusters through measurements of magnetic field fluctuations," presented at the 30th International Electric Propulsion Conference, Florence, Italy, 2007, IEPC-2007-143.

[15]R. R. Hofer, I. G. Mikellides, I. Katz, and D. M. Goebel, "Wall sheath and electron mobility modeling in hybrid-PIC Hall thruster simulations," presented at the 43rd AIAA Joint Propulsion Conference & Exhibit, Cincinnati, OH, 2007, AIAA-2007-5267.

[16]I. D. Kaganovich, Y. Raitses, and D. Sydorenko, "Electron kinetic effects and beam-related instabilities in Hall thrusters," presented at the 43rd AIAA Joint Propulsion Conference & Exhibit, Cincinnati, OH, 2007, AIAA-2007-5206.

[17]M. K. Scharfe, C. A. Thomas, D. B. Scharfe, N. Gascon, M. A. Cappelli, and E. Fernandez, "Shear-based model for electron transport in 2D hybrid Hall thruster simulations," presented at the 43rd AIAA Joint Propulsion Conference & Exhibit, Cincinnati, OH, 2007, AIAA-2007-5208.

[18]A. Ducrocq, J. C. Adam, A. Heron, and G. Laval, "High-frequency electron drift instability in the cross-field configuration of Hall thrusters," *Phys. Plasmas*, 13, 2006, pp. 102111.

[19]F. Taccogna, R. Schneider, S. Longo, and M. A. Cappelli, "Fully kinetic 2D{r,θ} model of a Hall discharge," presented at the 43rd AIAA Joint Propulsion Conference & Exhibit, Cincinnati, OH, 2007, AIAA-2007-5211.

[20]N. B. Meezan, and M. A. Cappelli, "Kinetic study of wall collisions in a coaxial Hall discharge," *Phys. Rev. E*, 66, 2002, pp. 036401.

[21]Y. Raitses, D. Staack, M. Keidar, and N. J. Fisch, "Electron-wall interaction in Hall thrusters," *Phys. Plasmas*, 12, 2005, pp. 057104.

[22]J. M. Haas, A. D. Gallimore, K. McFall, and G. Spanjers, "Development of a high-speed, reciprocating electrostatic probe system for Hall thruster interrogation," *Rev. Sci. Instr.*, 71 (11), 2000, pp. 4131.

[23]W. A. Hargus, and M. A. Cappelli, "Laser-induced fluorescence measurements of velocity within a Hall discharge," *Appl. Phys. B*, 72, 2001, pp. 961-969.

[24]J. H. Malmberg, and J. S. deGrassie, "Properties of nonneutral plasma," *Phys. Rev. Lett.*, 35 (9), 1975, pp. 577.

[25]J. S. deGrassie, and J. H. Malmberg, "Waves and transport in the pure electron plasma," *Phys. Fluids*, 23 (63), 1980,

[26]E. H. Chao, R. C. Davidson, S. F. Paul, and K. A. Morrison, "Effects of background gas pressure on the dynamics of a nonneutral electron plasma confined in a Malmberg-Penning trap," *Phys. Plasmas*, 7 (3), 2000, pp. 831-838.

[27]J. Espejo, J. Quraishi, and S. Robertson, "Experimental measurement of neoclassic mobility in an annular Malmberg-Penning trap," *Phys. Rev. Lett.*, 84 (24), 2000, pp. 5520-5523.

[28]S. Robertson, and B. Walch, "Electron confinement in an annular Penning trap," *Phys. Plasmas*, 7 (6), 2000, pp. 2340-2347.

[29]S. Robertson, J. Espejo, J. Kline, Q. Quraishi, M. Triplett, and B. Walch, "Neoclassical effects in the annular Penning trap," *Phys. Plasmas*, 8 (5), 2001, pp. 1863-1869.

[30]R. C. Davidson, *Physics of Nonneutral Plasmas,* Imperial College Press and World Scientific Publishing Co. Pte. Ltd, London, UK, 2001.

[31]E. C. Fossum, and L. B. King, "An Electron Trap for Studying Cross-field Mobility in Hall Thrusters," IEEE Transactions on Plasma Science, Special Issue on Plasma Propulsion (accepted for publication: Mar. 12, 2008; publication date: Aug., 2008)

[32]J. A. Linnell, and A. D. Gallimore, "Internal plasma potential measurements of a Hall thruster using xenon and krypton propellant," *Phys. Plasmas*, 13, 2006, pp. 093502.
[33]Maxwell ® SV, (2005, Nov. 30) www.ansoft.com/maxwellsv
[34]CPAT and Kinema Software. (2007, May 19). The Siglo Database [Online]. Available: http://www.siglo-kinema.com
[35]A. R. Hutson, "Velocity analysis of thermionic emission from single-crystal tungsten," *Phys. Rev.*, 98 (4), 1955, pp. 889.
[36]I. H. Hutchinson, *Principles of Plasma Diagnostics, 2nd Edition,* Cambridge University Press, Cambridge, UK, 2002.
[37]H. Himura, C. Nakashima, H. Saito, and Z. Yoshida, "Probing of flowing electron plasmas," *Phys. Plasmas*, 8 (10), 2001, pp. 4651-4658.
[38]J. P. Kremer, T. Sunn Pedersen, Q. Marksteiner, R. G. Lefrancois, and M. Hahn, "Diagnosing pure-electron plasmas with internal particle flux probes," *Rev. Sci. Instr.*, 78, 2007, pp. 013503.